

# Impact of apolipoprotein A1 on tumor immune microenvironment, clinical prognosis and genomic landscape in hepatocellular carcinoma

Ying Wang<sup>1,2,3,§</sup>, Shipeng Chen<sup>4,§</sup>, Xiao Xiao<sup>1,§</sup>, Fan Yang<sup>5</sup>, Jinhan Wang<sup>6</sup>, Hui Zong<sup>3,7</sup>, Yuzhen Gao<sup>8</sup>, Chenjun Huang<sup>1</sup>, Xuewen Xu<sup>1</sup>, Meng Fang<sup>2</sup>, Xiaoyan Zhang<sup>3,\*</sup> and Chunfang Gao<sup>1,\*</sup>

<sup>1</sup>Clinical Laboratory Medicine Center, Yueyang Hospital of Integrated Traditional Chinese and Western Medicine, Shanghai University of Traditional Chinese Medicine, Shanghai 200437, China

<sup>2</sup>Department of Laboratory Medicine, Shanghai Eastern Hepatobiliary Surgery Hospital, Shanghai 200438, China

<sup>3</sup>Research Center for Translational Medicine, Shanghai East Hospital, School of Life Sciences and Technology, Tongji University, Shanghai 200092, China

<sup>4</sup>Department of Medical Microbiology and Infection Prevention, Tumor Virology and Cancer Immunotherapy, University Medical Center Groningen, University of Groningen, Groningen 9712 CP, The Netherlands

<sup>5</sup>State Key Laboratory for Diagnosis and Treatment of Infectious Diseases, The First Affiliated Hospital, School of Medicine, Zhejiang University, Hangzhou 310058, China

<sup>6</sup>Department of Hepatobiliary and Pancreatic Surgery, Shanghai East Hospital, Tongji University School of Medicine, Shanghai 200120, China

<sup>7</sup>Institutes for Systems Genetics, Frontiers Science Center for Disease-Related Molecular Network, West China Hospital, Sichuan University, Chengdu 610041, China

<sup>8</sup>Department of Clinical Laboratory, Sir Run Run Shaw Hospital, Zhejiang University School of Medicine, Hangzhou 310058, China

\*Correspondence: Chunfang Gao, [gaocf1115@163.com](mailto:gaocf1115@163.com); Xiaoyan Zhang, [xyzhang@tongji.edu.cn](mailto:xyzhang@tongji.edu.cn)

<sup>§</sup>Ying Wang, Shipeng Chen, and Xiao Xiao contributed equally to this work.

## Abstract

**Background:** Current knowledge on apolipoprotein A1 (APOA1) in hepatocellular carcinoma (HCC) is fragmented and even contradictory. Multi-dimensional analyses are required to comprehensively elucidate its value and underlying mechanism.

**Methods:** We collected 49 RNA-seq datasets, 40 cell line types data and 70 scRNA pan-cancer datasets public available, including 17 HCC datasets (1754 tumor samples), and enrolled 73 pairs of HCC tissue and 516 blood samples independently from our clinics. APOA1 impacting on the HCC tumor microenvironment (TME) was analyzed using intensive data mining. Methylation sequencing, flow cytometry, quantitative PCR, western blot, immunohistochemistry and clinical chemistry assays were conducted for wet experimental investigation.

**Results:** The APOA1 ontology fingerprint indicated that it played various crucial biological roles in HCC, primarily involved in cholesterol efflux. Consistent findings at histology, serology, and clinical follow-up revealed that high APOA1 was a good prognosis indicator of HCC. Hypermethylation in the APOA1 promoter region was found in clinical samples which is in accordance with the reduction of APOA1 in HCC. The cell cycle, DNA replication, mismatch repair pathways, and tumor cell proliferation were less observed in the HCC APOA1<sup>high</sup> subgroup. The favorable immunoregulatory abilities of APOA1 showed interesting findings: a positive correlation between APOA1 and anti-tumor immune cells (NK, CD8<sup>+</sup> T cells) and a negative association with immune cells exerting immunosuppressive effects, including M2 macrophages.

**Conclusion:** This is an integrative multidimensional exploration of APOA1 using bioinformatics and experiments. Both the prognostic value and anti-tumor effects based on APOA1 panoramic exploration in the HCC TME demonstrate a new potential clinical target for HCC assessment and intervention in the future.

**Keywords:** APOA1, HCC, prognosis, tumor microenvironment, immune cells, NK cell

## Introduction

Hepatocellular carcinoma (HCC) is the fourth most common cause of cancer mortality in the world, accounting for ~800 000 deaths every year.<sup>1,2</sup> Although current therapies such as liver resection, ablation, and liver transplantation have improved HCC management, the clinical outcomes are not so satisfying, with limited long-term survival, especially in HCC patients with intermediate and advanced stages.<sup>3</sup> The prognostic indicators play a pivotal role in monitoring tumor recurrence and improving the prognosis of patients.<sup>4</sup> Although numerous efforts have been

made to predict HCC prognosis, specific prognostic indicators are still lacking.<sup>5,6</sup> In addition, research for developing additional novel therapeutic agents could potentially augment the presently available treatments. Therefore, it is imperative to develop potential prognostic and therapeutic targets for improving the prognosis and treatment of HCC.

Apolipoprotein A1 (APOA1), a protein mainly produced by the liver, constitutes ~70% of high-density lipoprotein. It is regarded as a key liver function parameter as well as a lipid metabolism related molecule. A serum proteomics study of patients with

Received: July 20, 2023. Accepted: August 30, 2023. Published: 2 September 2023

© The Author(s) 2023. Published by Oxford University Press on behalf of the West China School of Medicine & West China Hospital of Sichuan University. This is an Open Access article distributed under the terms of the Creative Commons Attribution-NonCommercial License (<https://creativecommons.org/licenses/by-nc/4.0/>), which permits non-commercial re-use, distribution, and reproduction in any medium, provided the original work is properly cited. For commercial re-use, please contact [journals.permissions@oup.com](mailto:journals.permissions@oup.com)

chronic liver disease demonstrated that a lower level of APOA1 posed a risk for the development of HCC.<sup>7</sup> The serum APOA1 level was significantly lower in HCC patients with advanced stages and tumor recurrence compared to patients with remission.<sup>8,9</sup> In addition, patients with elevated concentrations of pre-treatment serum APOA1 experienced better survival.<sup>8</sup> These findings indicate that APOA1 might hold potential as a novel serum marker for monitoring the prognosis of HCC.

Intriguingly, clinical studies have demonstrated that APOA1 has a protective effect against HCC, but the mechanisms remain uncertain. Besides, the mechanisms underlying the transcriptional suppression of APOA1 in HCC tumor tissue is less investigated. Researchers have attempted to elucidate the protective function of APOA1 against cancer development. For example, *in vitro* assays demonstrated that APOA1 could suppress the proliferation of HCC cells by arresting the cell cycle and promoting apoptosis.<sup>8</sup> However, no major direct inhibitory effect of APOA1 on tumor cells has been reported. For instance, no significant changes were observed in terms of cellular proliferation, various cell cycle parameters, or apoptosis rate when melanoma cells were treated with APOA1.<sup>10</sup> Additionally, an APOA1 mimetic peptide was unable to cause pancreatic cancer cells apoptosis or directly decrease tumor cell invasion and proliferation.<sup>11</sup> These contradictory findings regarding the direct influence of APOA1 on cancer cells indicate that the potential protective mechanisms of APOA1 are still controversial and remain unresolved.

In addition to cancer cells, the tumor microenvironment (TME), as an intricate cellular ecosystem, plays a prominent role in malignant growth and metastasis.<sup>12,13</sup> Within the TME, numerous immune cells are related to the establishment of an immunosuppressive TME to promote tumor progression, including M2 macrophages, myeloid-derived suppressor cells (MDSCs), and cancer-associated fibroblasts (CAFs). Meanwhile, cytotoxic CD8<sup>+</sup> T cells, M1 macrophages and natural killer (NK) cells can mount an effective antitumor response.<sup>12,14</sup> Accordingly, increasing the infiltration of cytotoxic CD8<sup>+</sup> T and NK cells, as well as reprogramming immunosuppressive M2 macrophages into M1 with antitumor phenotype, would lead to better immunotherapeutic efficacy.<sup>12,15</sup> Although APOA1, or its mimetic peptide, has no direct effect on tumor cells, a previous study indicated that it can mediate the regression of established tumors and reduce tumor metastasis in animal models.<sup>10</sup> Therefore, this study hypothesized that the antineoplastic activity of APOA1 may not only be derived from its direct impact on tumor cells but also its influence on the immune cells in the TME.

The current clinical studies on APOA1 provide fragmented information, and, to the best of our knowledge, a comprehensive assessment of APOA1 as a potential prognostic and therapeutic target has not been performed. In the current study, we collected the bulk RNA and single-cell RNA sequencing (scRNA-seq) public data from HCC samples to investigate the influence of APOA1 on both tumors and TME. Then the gene and protein expression of APOA1 in HCC tumor tissues, as well as adjacent normal tissues, were carefully validated and evaluated by a series of bench experiments. The DNA methylation levels at single-CpG resolution were further investigated to explore the possible mechanisms that lead to APOA1 reduction in HCC tumor tissue. Additionally, a pan-cancer analysis of APOA1 expression was performed to examine its specificity and the prognostic surveillance value of APOA1 in HCC. Altogether, the present study performed a systematic and comprehensive evaluation of APOA1 as a potential prognostic indicator of HCC as well as investigating its protective role

against tumors based on a landscape analysis of the TME in HCC patients.

## Method

### Datasets and collection of HCC samples

#### Public data

In detail, text-mining data were collected from the PubMed database. Omics data were derived from The Cancer Genome Atlas (TCGA), International Cancer Genome Consortium (ICGC) and Gene Expression Omnibus (GEO) databases. The quantification analysis of infiltrated immune cells in the TME was based on 12 datasets from the GEO database, 2 sets of RNA-seq from TCGA-LIHC project (liver cancer) and the ICGC LIRI-JP project (liver cancer), and a set of cancer scRNA-seq data from the GEO database. Detailed descriptions of the included datasets are listed in [supplementary Table S1](#), see online [supplementary material](#).

#### Clinical samples collection

Samples for experimental validation were all obtained from the Eastern Hepatobiliary Surgery Hospital (EHBH), including 20 pairs of HCC tissues and adjacent normal tissues for quantitative PCR (qPCR), 8 pairs of HCC tissues and adjacent normal tissues for western blot (WB) and bisulfite amplicon sequencing (BSAS), and a tissue chip containing 45 pairs of HCC and adjacent normal tissues for immunohistochemistry (IHC) analysis. In addition, 516 blood samples (332 HCC patients and 184 healthy donors) were obtained to detect the level of APOA1. Among these, flow cytometry was used to quantify CD3<sup>+</sup>CD16<sup>+</sup>/CD56<sup>+</sup> and CD8<sup>+</sup> T cells in 300 HCC samples. Detailed descriptions of the included datasets are listed in [supplementary Table S2](#), see online [supplementary material](#).

### Construction of the APOA1 ontology fingerprint in pan-cancer

Based on the collected literature of 33 different tumor types, we used the explainable gene ontology fingerprint (XGOF) method developed by our previous study<sup>16</sup> to establish the XGOF of APOA1 in pan-cancer. For each tumor, APOA1-Gene Ontology (GO) term pairs were extracted with an adjusted *P* value < 0.05 as the threshold and were defined as the gene fingerprint of APOA1.

### Analysis of APOA1 expression and the infiltration fraction of cell subsets in the TME

We calculated the correlation between APOA1 expression and the infiltration fraction of cell subsets in HCC, and the tumor purity was corrected by TIMER2. Cell infiltration fraction scores methods include XCELL, CIBERSORT, EPIC, TIMER, MCPOUNTER, CIBERSORT\_ABS, and QUANTISEQ. Six immune subtypes (C1–C6) in HCC TME are defined by Thorsson *et al.*<sup>17</sup> This study mainly focused on C1–C4 immune subtypes, in which C1 stands for wound healing, C2 represents Interferon (IFN)- $\gamma$  dominant, C3 indicates inflammation, and C4 means lymphocyte depleted.

### Validation at RNA and protein levels

#### qPCR

qPCR was performed using a 7900HT Fast Real-Time PCR System (Life Technology, USA). PCR primers were designed using Primer Premier 6.0 software. The forward primer sequence of APOA1 is 5'-CTAAAGCTCCTTGACAAGCTGGG-3' and the reverse primer sequence is 5'-TTTCCAGGTTATCCAGAAGCTC-3'.

## WB

The total protein of tissue was extracted by protein lysis solution (Beyotime Biotechnology Co., Ltd., Beijing). The protein extraction concentration was detected by using a BCA Protein Assay kit (Thermo Fisher, USA). Total protein (40  $\mu$ g) was separated by 12% Sodium Dodecyl Sulfate-polyacrylamide Gel Electrophoresis (SDS-PAGE) and then transferred to a PVDF membrane (Millipore, USA). After blocking with 5% nonfat milk for 1 h, the membrane was incubated overnight at 4°C with primary antibodies (ab52945, Abcam, UK). After incubation with Horseradish Peroxidase (HRP)-conjugated secondary antibodies for 1 h at room temperature, blots were developed by using Enhanced Chemiluminescence (ECL) luminescence reagent (Thermo Fisher, USA). The relative expression level of APOA1 was normalized by the level of Glyceraldehyde-3-phosphate Dehydrogenase (GAPDH). Quantitative analysis was performed using Image J.

## IHC analysis

Primary monoclonal antibodies against APOA1 (ab52945, Abcam, UK, 1:100) were applied to the 45 paired samples of tumor and adjacent normal tissues, formalin-fixed and paraffin-embedded on a tissue microarray (TMA) (Shanghai Outdo Biotech Co., Ltd.). TMA was automatically scanned using the Tissue FAXS imaging system (TissueGnostics, Vienna, Austria), and reconstituted virtual slides were subjected to quantitative image analysis. Analysis was performed using StrataQuest (v. 7.1.1.119; TissueGnostics). StrataQuest analysis software can be used to obtain the grayscale map of different color channels. A nuclear segmentation algorithm was applied to the nucleus channel to identify individual cells. Then, the expression of APOA1 marker was computed for every cell identified. Scatterplots of intensity and area were created to enumerate the number of positive and negative cells for APOA1 marker.

## BSAS

The methylation level in the promoter region of APOA1 was verified by BSAS in 8 HCC patients. The probes were designed based on the APOA1 gene promoter region from TCGA DNA methylation sequencing data of HCC, including sites 26 (11: 116 708 224), 55 (11: 116 708 253), 101 (11: 116 708 299), 118 (11: 116 708 316), 131 (11: 116 708 329) and 215 (11: 116 708 413) (supplementary Table S3, see online supplementary material). The raw data was quality controlled by FastQC software. Filtered clean reads used Bismark running with bowtie2 for alignment with the reference sequence with default parameters. Using the meth.call function in the R package methylKit, the methylation of each CpG cytosine was extracted to further calculate the cytosine methylation level. The methylation ratio of all CpG cytosines was computed in the target fragment of each sample.

## Detection of APOA1 level and immunophenotyping of immune cells in the blood

The APOA1 level (mg/dl) was obtained using standard methods and matched reagents on a Roche Modular P800 Chemistry Analyzer (Roche, Basel, Switzerland). Monoclonal antibodies anti-CD3<sup>+</sup>/CD8<sup>+</sup> and anti-CD3<sup>+</sup>/CD16<sup>+</sup>/CD56<sup>+</sup> were used to evaluate CD8<sup>+</sup> T cells and NK cells using flow cytometry, respectively.

## Cell proliferation experiment

For the proliferation assay, HCC-LM3 cells were aliquoted into a 96-well plate at 5000/100  $\mu$ l per well with 100  $\mu$ l of Dulbecco's

Modified Eagle Medium (DMEM) containing 10% Fetal Bovine Serum (FBS). After 24 h, cells were treated with different concentrations of recombinant APOA1 (0, 2.5, 5, 10, or 15  $\mu$ g/ml) and exposed to APOA1 for 48 h. At the indicated time points, cell counting kit 8 (CCK-8) solution (MedChemExpress, China) was added to determine the number of viable cells in each well.

## Statistical analyses

Student's t-test and Mann-Whitney U test were performed with Prism 8.0 (GraphPad). A P-value < 0.05 (\*P < 0.05, \*\*P < 0.01, \*\*\*P < 0.005, \*\*\*\*P < 0.001) was considered statistically significant. Survival analysis was performed (Gehan-Breslow test) to compare OS among multiple groups. In descending order (e.g. APOA1 expression level), the top 50% was defined as the APOA1<sup>high</sup> group, and the bottom 50% was the APOA1<sup>low</sup> group.

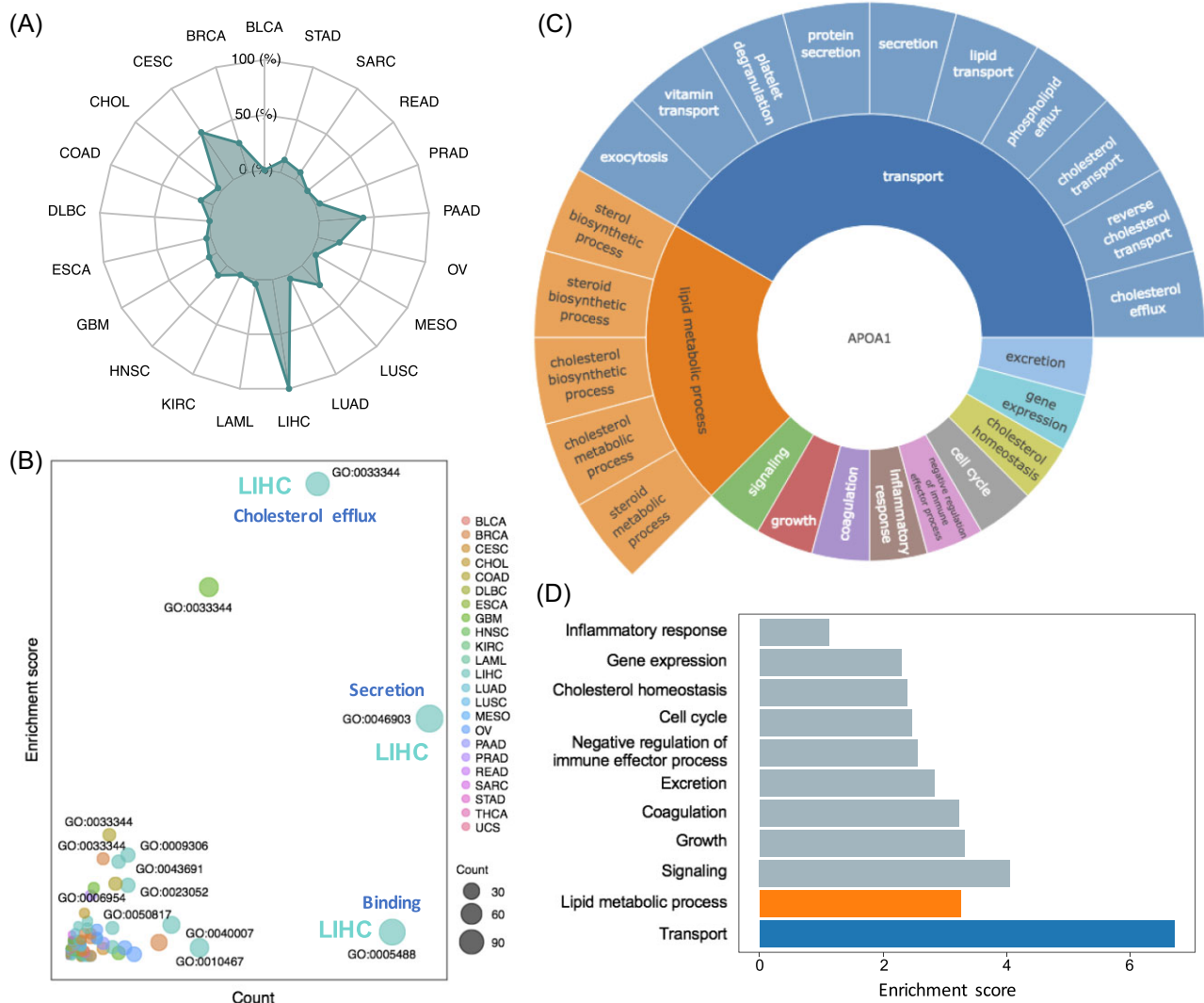
## Results

### Pan-cancer analysis of XGOF of APOA1

The APOA1 gene fingerprint was constructed in 23 different types of tumors, according to 2 743 077 published studies. Supplementary Figure S1 (see online supplementary material) presents APOA1-related GO terms enriched in three GO categories, including 49 biological processes, 9 molecular functions, and 14 cellular component terms. Figure 1A shows the distribution of APOA1-related GO terms in different types of tumors, demonstrating the crucial biological importance of APOA1 in liver cancer. Cholesterol efflux (GO: 0 033 344) is the most important function related to APOA1 in most malignancies, especially in HCC (Fig. 1B). In addition, Fig. 1C shows more details regarding the enrichment of APOA1 in biological process GO terms in liver cancer. Based on GO hierarchical relationships, most biological process GO terms belong to the transport and lipid metabolism process category. The enrichment scores of APOA1-GO term pairs in Fig. 1D, according to the liver cancer literature, indicate that APOA1 is mainly involved in transport during tumor development, as well as signaling, inflammatory response, lipid metabolic process, gene expression, cell cycle, negative regulation of immune effector process, excretion, growth, cholesterol homeostasis, and coagulation. Overall, these results show that APOA1 plays various crucial biological roles in liver cancer.

### Specific expression of APOA1 in liver

Next, the expression of the APOA1 gene in various cell lines was evaluated. The 1457 samples from 40 cell line types from the Cancer Cell Line Encyclopedia (CCLE) database demonstrated that APOA1 gene expression was quite specific to liver cells (Supplementary Figure S2A, see online supplementary material). Furthermore, the interactive body map using TCGA and Genotype-Tissue Expression (GTEx) datasets showed that the expression distribution of the APOA1 gene was organ-specific, with a lower median expression in liver tumor tissues ( $n = 371$ , APOA1 value = 6017.3) compared to that in normal tissues ( $n = 160$ , APOA1 value = 8495.76) (Figure S2B). Datasets from the TCGA pan-cancer data (34 tumor types,  $n = 12 557$ ) further validated the liver-specific expression of the APOA1 gene, suggesting that APOA1 gene expression was significantly lower in HCC compared with that in normal liver tissues (Fig. 2A). To further validate these findings, 20 pairs of HCC tissues and adjacent normal tissues were acquired to measure the mRNA expression of APOA1, and it was demonstrated that APOA1 expression was, indeed, considerably reduced in HCC tissues ( $P < 0.005$ ,



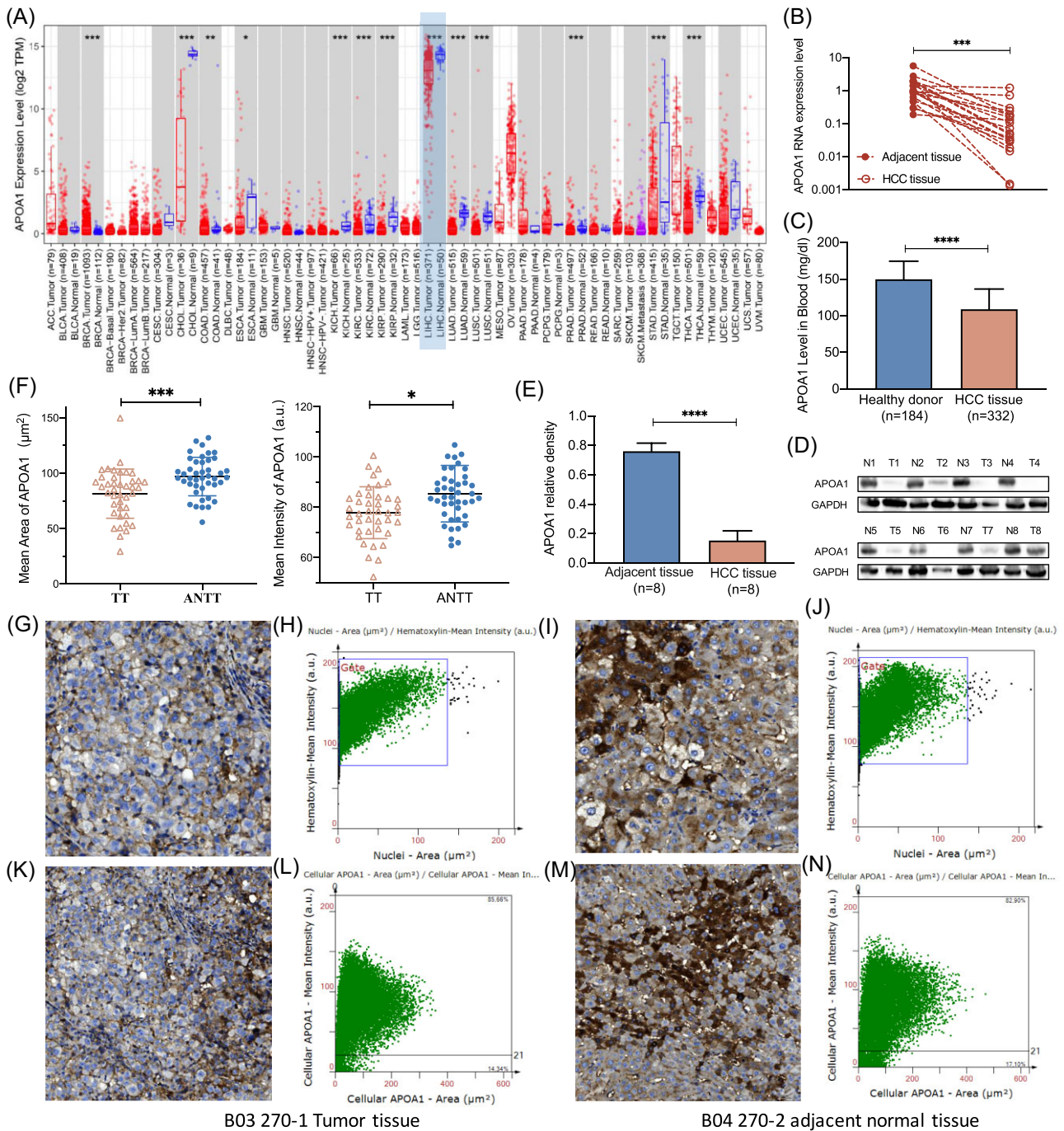
**Figure 1.** Gene ontology fingerprint of APOA1. **(A)** Number of GO terms reported by APOA1 in different tumor studies; the enrichment significance P-value of APOA1-GO term pairs was  $<0.05$ . **(B)** Enrichment of APOA1-GO term pairs in different tumor studies. Size represents the number of APOA1-GO term pairs that co-occur in the same sentence, and the y-axis represents the enrichment score of these pairs in the published literature for each tumor type. **(C)** APOA1 gene fingerprint of biological processes in liver cancer. The biological processes of APOA1 enrichment in HCC were classified into three major categories based on GO level results, including transport, lipid metabolism processes, and others. **(D)** Enrichment analysis of the biological process fingerprint of APOA1. GO terms related to transport or lipid metabolism processes shown in (C) were merged into their parent category, respectively. The x-axis indicates the enrichment score of each biological process GO term-APOA1 pair in liver cancer literature.

Fig. 2B). The APOA1 level in blood was also measured based on a large EHBH cohort, which demonstrated that the level of APOA1 in serum was significantly lower in HCC patients compared to healthy donors (Fig. 2C). Additionally, the same notable down-regulation was observed at the protein level. WB experiments confirmed that the level of APOA1 protein in tumor tissues was much lower than that in adjacent normal tissues ( $P < 0.0005$ , Fig. 2D,E). Furthermore, IHC revealed that APOA1 was greatly reduced in HCC. Compared with the mean positive intensity and mean positive area, the APOA1 level of adjacent normal tissues was higher than that of cancerous tissue, with P values of 0.024 and 0.0004, respectively (Fig. 2F-N). Taken together, this clearly suggests that APOA1 is expressed specifically in the liver and that tumor tissues express much less APOA1 than healthy donors.

### High methylation level of APOA1 promoter region in HCC

To investigate whether the low expression of APOA1 in HCC is related to hypermethylation of its promoter region, APOA1 CpG methylation levels were searched in 17 different liver cancer cell lines from the Depmap database. It was found that the promoter region of APOA1 (e.g. 11:116 708 299, 11: 116 708 316) is hypermethylated in most liver cancer cell lines (Fig. 3A). Of note, APOA1 expression and methylation levels were significantly negatively correlated in tumor samples (Fig. 3B,  $r = -0.61$ ,  $P < 2.2e-16$ ), but not in normal samples ( $r = -0.19$ ,  $P = 0.24$ ). This was further validated by BSAS detection based on the probe position information of the TCGA-LIHC DNA methylation dataset. The RNA expression level of APOA1 by qPCR was negatively correlated with the methylation levels of six sites in the APOA1 promoter





**Figure 2.** Intrinsic difference of APOA1 expression between HCC tissue and adjacent normal tissue. **(A)** Expression of APOA1 gene among different tumors in the TCGA database based on RNA-seq data; light blue background represents the HCC dataset. **(B)** qPCR experiment of APOA1 in HCC ( $n = 20$ ) tissues. The left dots represent control samples and the right dots represent tumor samples. \* $P < 0.05$ , \*\* $P < 0.005$ , \*\*\* $P < 0.0005$ , \*\*\*\* $P < 0.0001$  (Mann-Whitney U test). **(C)** Comparison of APOA1 levels (mg/dl) in blood samples collected from EHBH. HCC samples are on the left (blue) and healthy donors are on the right (orange). **(D)** WB experiment of APOA1 in HCC ( $n = 8$ ) tissues. **(E)** Grayscale analysis of APOA1 protein for WB bands. **(F)** IHC experiment of APOA1 expression in HCC. Left: mean area ( $\mu\text{m}^2$ ); the total area from APOA1-positive staining of positive cells divided by the number of positive cells. Right: mean intensity (a.u., arbitrary unit); the total intensity from APOA1 positive staining of positive cells divided by the number of positive cells. **(G-N)** IHC staining and Tissue Gnostics (TG) scatter diagrams of cancer/adjacent normal tissue sections of a representative patient (No. 270). (G, I) High-power lens, (K, M) low-power lens, and (H, J) analysis result of the nuclear area and hematoxylin staining intensity. We circled the gate to remove small cells/cell debris, and the cells analyzed in (L, N) were derived from the gate in (H, J) diagram. To remove non-specific staining, the cut-off value of average intensity is 21.

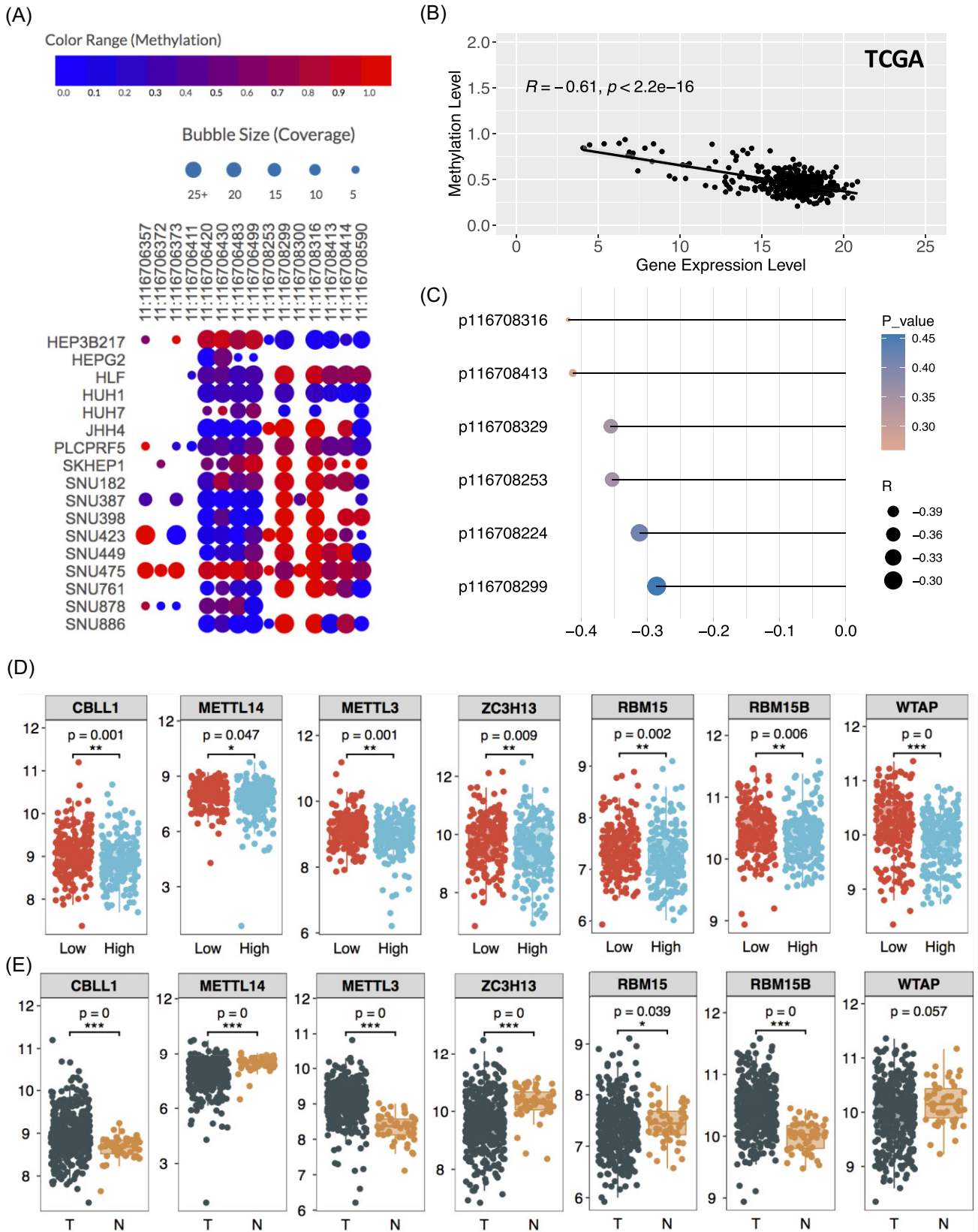


**Figure 3.** Methylation level of APOA1 promoter region in HCC. **(A)** APOA1 CpG methylation level in liver cancer cell lines derived from the Demap database. **(B)** Correlation analysis of the APOA1 expression level and methylation level based on HCC samples from TCGA (LIHC project). R was calculated using the Pearson coefficient method. **(C)** Lollipop plot of the correlation between the methylation levels of six sites in the APOA1 promoter region detected by BSAS and the RNA expression level of APOA1 by qPCR. **(D)** Expression differences of methylase-related genes between ApoA1<sup>high</sup> and ApoA1<sup>low</sup> expression groups based on the TCGA-LIHC RNA-seq dataset (ApoA1<sup>high</sup>, top 50%; ApoA1<sup>low</sup>, bottom 50%). **(E)** Expression differences of methylase-related genes between tumor and adjacent normal groups based on the TCGA-LIHC RNA-seq dataset.



region, especially p116708316 and p116708413 (Fig. 3C,  $r \leftarrow -0.4$ ). In addition, the mRNA expression of m6A methylase-related genes between APOA1<sup>high</sup>/APOA1<sup>low</sup> expression groups and between tumor/normal groups based on the TCGA-LIHC dataset was also evaluated, respectively (Fig. 3D,E). The expression of methylase-related genes was lower in the APOA1<sup>high</sup> group, which may indirectly reflect the antitumor effect of APOA1. For example, patients with lower APOA1 have higher METTL3, which has been reported to promote the development of HCC.<sup>18</sup> These combined results showed a significant negative relationship between APOA1 expression and methylation level of the APOA1 promoter region in HCC tumor tissues.

### Prognostic value of APOA1 gene in HCC

To explore the value of the APOA1 gene as a prognostic marker for HCC, survival analysis between APOA1<sup>high</sup> and APOA1<sup>low</sup> patients with liver cancer classified by the median of APOA1 mRNA level was performed. The TCGA-LIHC dataset ( $n = 368$  tumor samples) showed that the overall survival (OS) of patients in the APOA1<sup>high</sup> group was significantly longer than that in the APOA1<sup>low</sup> group ( $P = 2e-04$ , Fig. 4A). Patients were further divided into four groups according to their Tumor Node Metastasis (TNM) stage, and it was found that patients at the early tumor stage had higher expression levels of APOA1 than those at the advanced stage (Fig. 4B). These discoveries were further confirmed based on another two independent patient cohorts (GSE14520,  $n = 242$ ; GSE15654,  $n = 150$ ) (Fig. 4C–E). Figure 4F revealed that expression of APOA1 was significantly higher in the survival group than in the death group. This suggested that the expression of APOA1 is related to favorable survival for liver cancer.

### APOA1 expression correlates with the infiltration of immune cells in the liver TME

The gene fingerprint of APOA1 revealed its association with immune modulation, which is understudied. Based on 70 scRNA datasets from public databases, the expression of APOA1 in different cells at single-cell resolution was assessed here. The scRNA pan-cancer data showed that APOA1 in different cell types was mainly expressed in HCC (Supplementary Figure S3A, see online supplementary material). In detail, the scRNA data of liver cancer showed that APOA1 was mainly expressed in hepatic progenitor cells, malignant cells, and immune cells, including monocytes, macrophages, NK and T cell proliferation (Figure S3B). In particular, APOA1 was mostly expressed in NK cells based on the smartseq2 scRNA-seq dataset (GSE140228, Fig. 5A,B). Moreover, to validate this discovery, a flow cytometry experiment was performed based on our EHBH cohort. It demonstrated that the proportion of NK cells in the APOA1<sup>high</sup> expression group was higher than that in the APOA1<sup>low</sup> group (Fig. 5C,  $n = 300$ ). HCC patients who had two consecutive laboratory tests were recruited for case exploration. It can be seen that the changing trend of APOA1 level is consistent with the changing proportion of NK cells (Fig. 5D). Furthermore, based on the GEO dataset (GSE128726) detecting the gene expression profile in NK cells, the expression of APOA1 in NK cells verified that APOA1 expression was significantly reduced in HCC groups compared with that in the healthy control group (Fig. 5E). According to APOA1 expression and NK cell infiltration scores, HCC patients were divided into three categories. Notably, the survival of patients with APOA1<sup>high</sup>NK<sup>high</sup> was significantly longer than that in the other groups, and the patients in the APOA1<sup>low</sup>NK<sup>low</sup> group had the worst OS (Fig. 5F). To evaluate the impact of APOA1 expression on NK cells, APOA1

was screened through the integrated CRISPR-CAS9 screen database (iCSDb) indicating the main effect on NK cell exposure (Supplementary Figure S4A, see online supplementary material). Furthermore, we found that APOA1 knockout mainly affects the cancer cell response to NK cells by screening the BioGRID database (Figure S4B).

Moreover, the relationship between APOA1 expression and the infiltration of immune cell subsets in the liver TME was further explored using published bulk RNA-seq and microarray datasets. Combining the consistency of several datasets and methodologies, the results of TIMER2 demonstrated that APOA1 expression in HCC was positively correlated with scores of NK cells, hematopoietic stem cells, and endothelial cells, but negatively correlated with Tregs, Th2 cells and mast cells (Supplementary Figure S5A, see online supplementary material). Bulk RNA-seq and scRNA-seq data both showed that APOA1 gene expression was correlated with the infiltration of various immune cells, although the expression of APOA1 in immune cells was not much higher in the scRNA dataset, except NK cells. Figures 6A,B showed that lymphocyte infiltration fraction and CD8<sup>+</sup> T cell score both increased in the APOA1<sup>high</sup> group, respectively. In addition, CD8<sup>+</sup> T cell marker genes, including CD8A, CD8B, GZMA, GZMB, and PRF1, all showed higher levels in the APOA1<sup>high</sup> group (Fig. 6C). HCC patients with two consecutive laboratory tests were again used for case exploration. Again, the changing trend of APOA1 level is consistent with the proportion of CD8<sup>+</sup> T cells (Fig. 6D). More interestingly, the TCGA samples were divided into APOA1<sup>high</sup> and APOA1<sup>low</sup> expression subgroups for immune subtype correlation analysis. The results suggested that the APOA1<sup>high</sup> group showed a lower wound healing score (Fig. 6E). In the macrophage cell subgroups, total macrophage and M2 macrophage cells in the APOA1<sup>high</sup> group were substantially decreased (Fig. 6F). Combined with Tumor Immune Dysfunction and Exclusion (TIDE) analysis, we found that APOA1 mRNA expression negatively correlates with CAF cells and MDSCs in HCC (Figure S5B).

The combined results imply that APOA1 is positively associated with immune cells that have antitumor activity while being negatively associated with immune cells that exert (underlying) immune suppression. In particular, the omics data and experiments both support the positive correlation between the expression of APOA1 and the infiltration level of NK cells.

### Differential pathways and mutation characteristics between APOA1<sup>high</sup> and APOA1<sup>low</sup> groups

To study the effect of APOA1 on tumor cells, we screened differentially expressed genes (DEGs) between APOA1<sup>high</sup> and APOA1<sup>low</sup> groups in two corpora of RNA-seq data and analyzed the enrichment pathways of DEGs. Figure 7A illustrates that DEGs in the APOA1<sup>high</sup> expression group were mainly enriched in metabolic pathways, while DEGs in the APOA1<sup>low</sup> expression group play a role in cell cycling, DNA replication, mismatch repair and other pathways. Consistently, dividing TCGA samples into APOA1<sup>high</sup> and APOA1<sup>low</sup> expression groups suggested that the APOA1<sup>high</sup> group had less tumor proliferation ( $P < 0.0001$ ) (Fig. 7B). To examine whether APOA1 stimulation influences HCC cell proliferation, a cell viability assay using CCK-8 was performed. Compared with negative control without APOA1 treatment, tumor cell viability treated with APOA1 was significantly suppressed in a dose-dependent manner after exposure to 2.5, 5, 10, or 15  $\mu\text{g/ml}$  APOA1 for 48 h (Fig. 7C). The expression of CD274 (PD-L1) was significantly decreased in the APOA1<sup>high</sup> group than

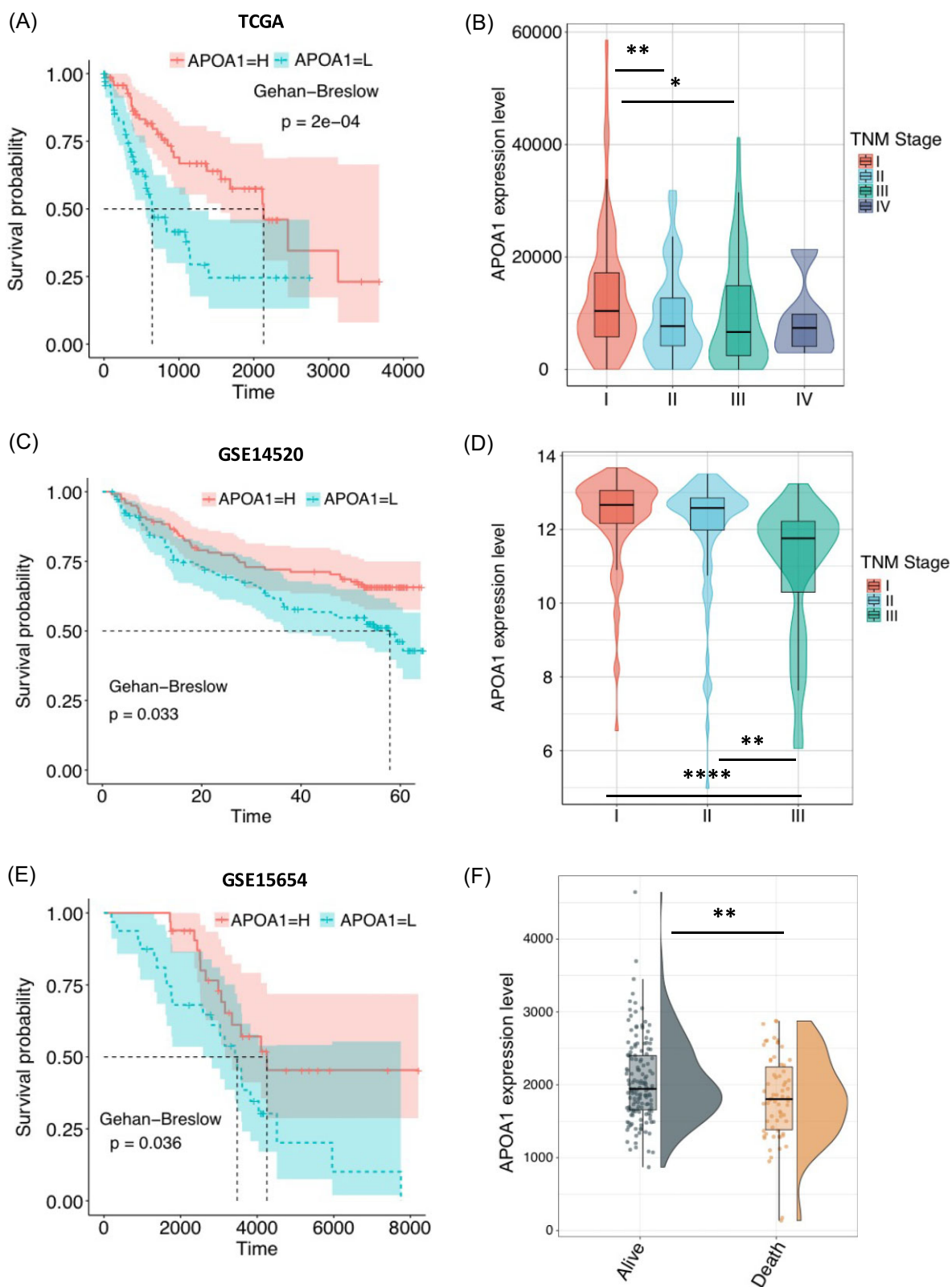


**Figure 4.** Diagnosis and prognosis value of APOA1 gene in HCC. **(A)** Survival analysis of patients in APOA1<sup>high</sup> and APOA1<sup>low</sup> expression groups using the TCGA cohort. **(B)** Difference of APOA1 expression in patients with different TNM stages based on TCGA clinical follow-up data. **(C)** Survival analysis of patients in APOA1<sup>high</sup> and APOA1<sup>low</sup> expression groups using the GSE14520 cohort. **(D)** Difference of APOA1 expression in patients with different TNM stages based on GSE14520 clinical follow-up data. **(E)** Survival analysis of patients in APOA1<sup>high</sup> and APOA1<sup>low</sup> expression groups using the GSE15654 cohort. **(F)** Difference of APOA1 expression based on survival status by the time of follow-up (alive or dead) using GSE15654 clinical follow-up data.



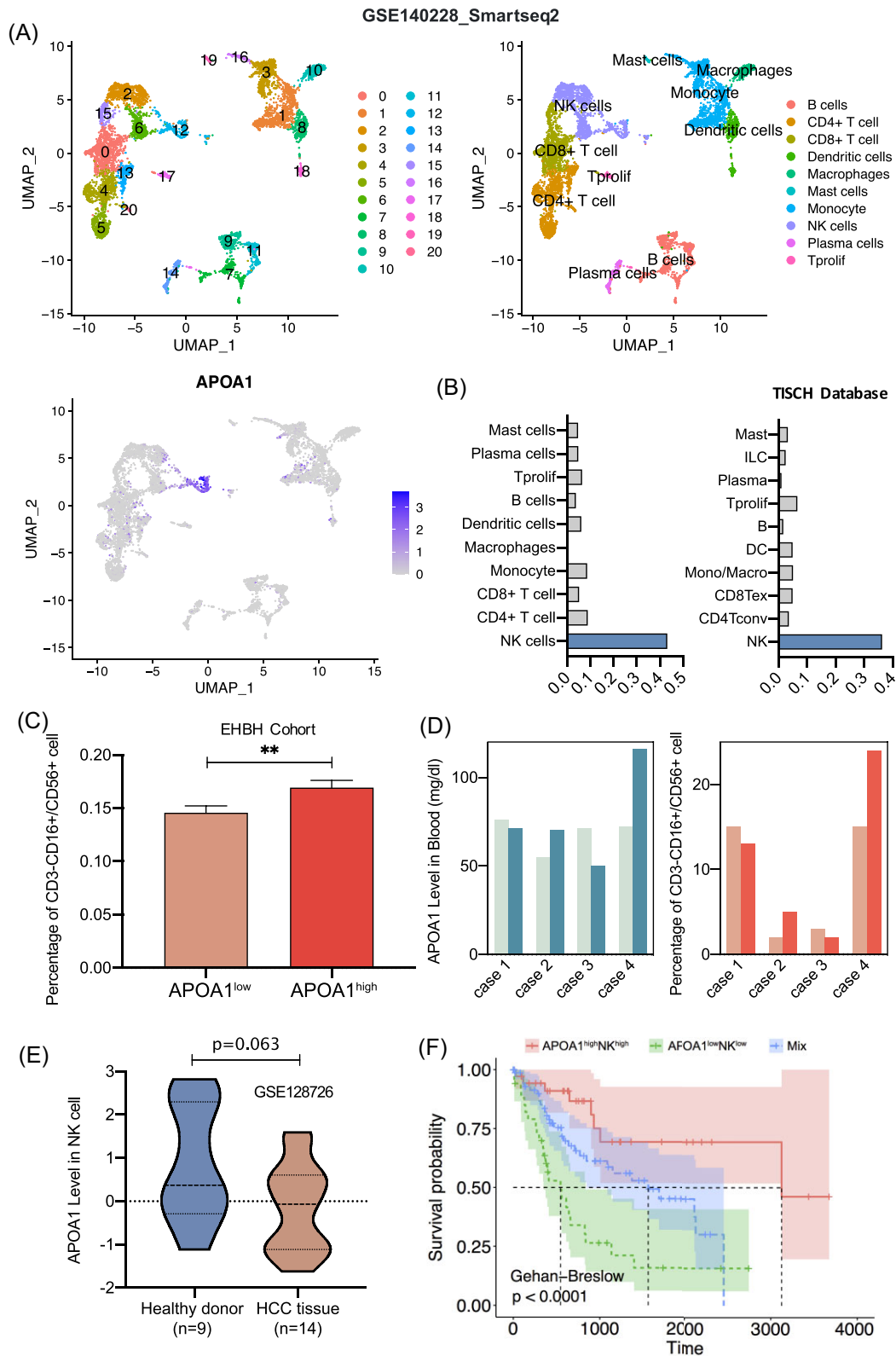


**Figure 5.** Association analysis of APOA1 expression and cell subtypes in HCC microenvironment. **(A)** UMAP plots of seurat cluster (left-top), cell annotation (right-top) and APOA1 expression (left-bottom) in HCC single-cell transcriptome sequencing data GSE140228. **(B)** The average expression level of APOA1 in different cell types (left: the analysis results of this study; right: the results of the TISCH database). **(C)** Changes in the proportion of NK cells between APOA1<sup>high</sup> and APOA1<sup>low</sup> groups in EHBH HCC blood samples. **(D)** Comparison of APOA1 level and proportion of NK cells in blood samples in four patients with HCC. The first detection point of cases 1, 3, and 4 is the preoperative time, and the second point is the recurrence time; the first detection point of case 2 refers to the first recurrence time, and the second point refers to the second recurrence time. **(E)** Comparison of APOA1 expression in NK cells between HCC patients and healthy donors using public dataset GSE128726. **(F)** Prognostic analysis of HCC patients based on the combination of APOA1 expression and NK cell infiltration score using TCGA-LIHC dataset. NK cell infiltration score was calculated by XCELL.

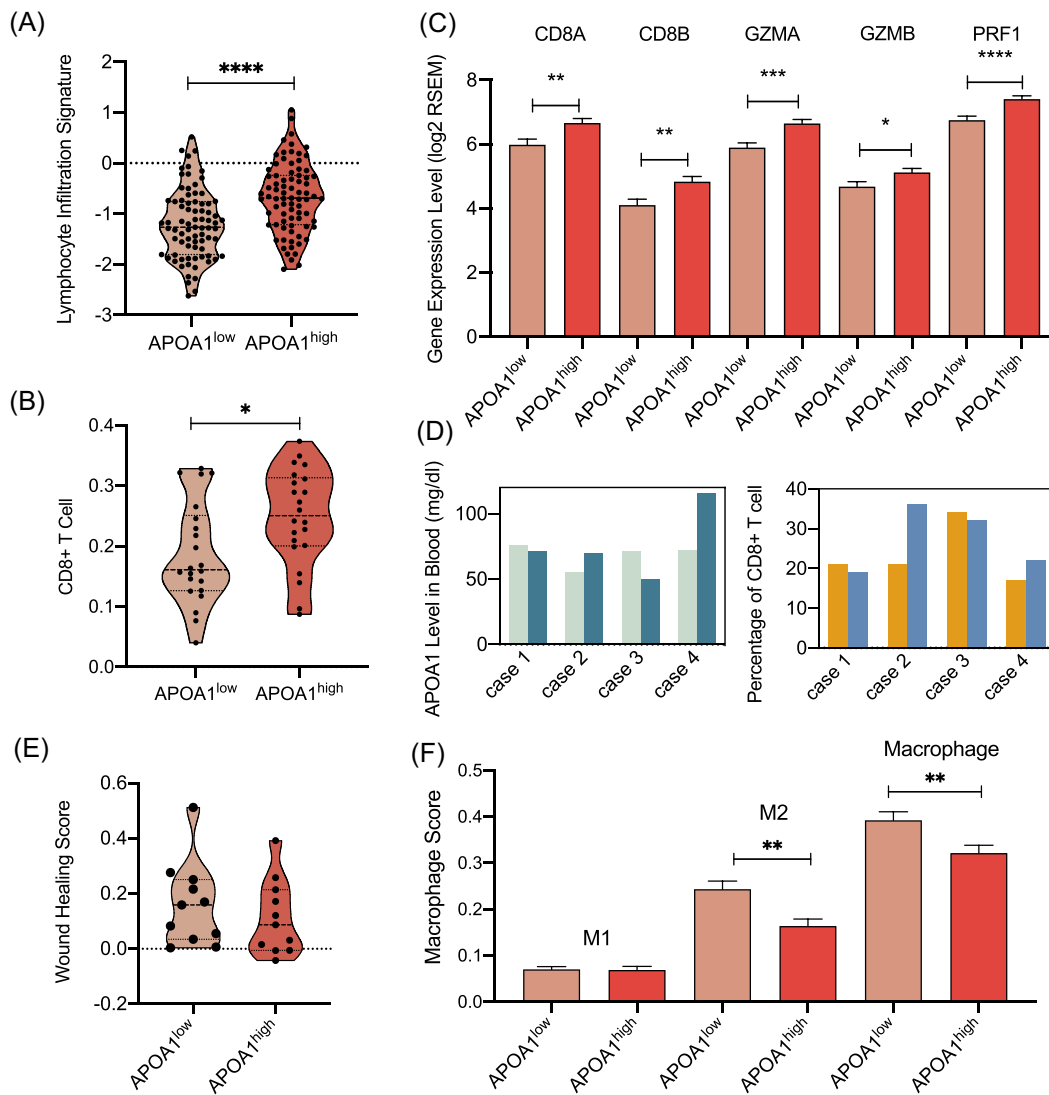


**Figure 6.** Relationship between APOA1 expression and the fraction of immune cells. (A) Difference in lymphocyte infiltration signature score was compared between APOA1<sup>high</sup> and APOA1<sup>low</sup> expression groups. (B) Difference in CD8<sup>+</sup> T cells scores was compared between APOA1<sup>high</sup> and APOA1<sup>low</sup> expression groups. (C) Difference in expression of CD8<sup>+</sup> T cell marker genes between APOA1<sup>high</sup> and APOA1<sup>low</sup> expression groups. (D) Comparison of APOA1 level and proportion of CD8<sup>+</sup> T cells in blood samples in four patients with HCC. (E) Difference of wound healing score in C1 subtype was compared between APOA1<sup>high</sup> and APOA1<sup>low</sup> expression groups using the TCGA-LIHC dataset. (F) Difference in infiltrating fractions of macrophage cells in C2 group between APOA1<sup>high</sup> and APOA1<sup>low</sup> expression groups.

that in APOA1<sup>low</sup> group (Fig. 7D). Mutation frequency (especially non-silent mutations, Fig. 7E) was decreased in the APOA1<sup>high</sup> group, which was consistent with our findings that APOA1<sup>low</sup> group genes were enriched in the mismatch repair pathway, as shown in Fig. 7A. These results indicate the direct antitumor effect of APOA1 on HCC.

## Discussion and conclusion

This study performed a landscape investigation including genomic, epigenetic, and proteomic analysis of APOA1, which provides clear evidence of the antitumor and immunomodulatory activity of APOA1 within the TME in patients with HCC. Along with the direct effect of APOA1 on cancer cells, its influence on adaptive and innate immune cells was also explored. Of note, the favorable effect of APOA1 on NK cells was discovered in this research. In addition, the role of APOA1 as a potential prognostic indicator of HCC was well studied. Moreover, the possible

mechanism due to hypermethylation that leads to APOA1 reduction in HCC tumor tissue was revealed. The functional impact of APOA1 on the prognosis and TME of HCC is summarized in Fig. 8.

First, the biological processes and molecular functions related to APOA1 were explored based on the large-scale text mining of millions of studies. It was found that APOA1 is largely involved in the process of transport and lipid metabolism and is associated with the development of HCC. It was observed that APOA1 expression was quite specific to the liver compared with other organs. Besides, the mRNA and protein expression of APOA1 is significantly lower in HCC tumor tissue compared to that in adjacent non-tumor tissue. Clinical samples further confirmed that HCC patients showed a significantly lower serum APOA1 level than healthy donors, and a lower serum APOA1 level was linked to poorer survival. To summarize, the liver-specific expression of APOA1, the distinction between normal liver and HCC tissues, and the consistency of serum and liver tissue results, was revealed.

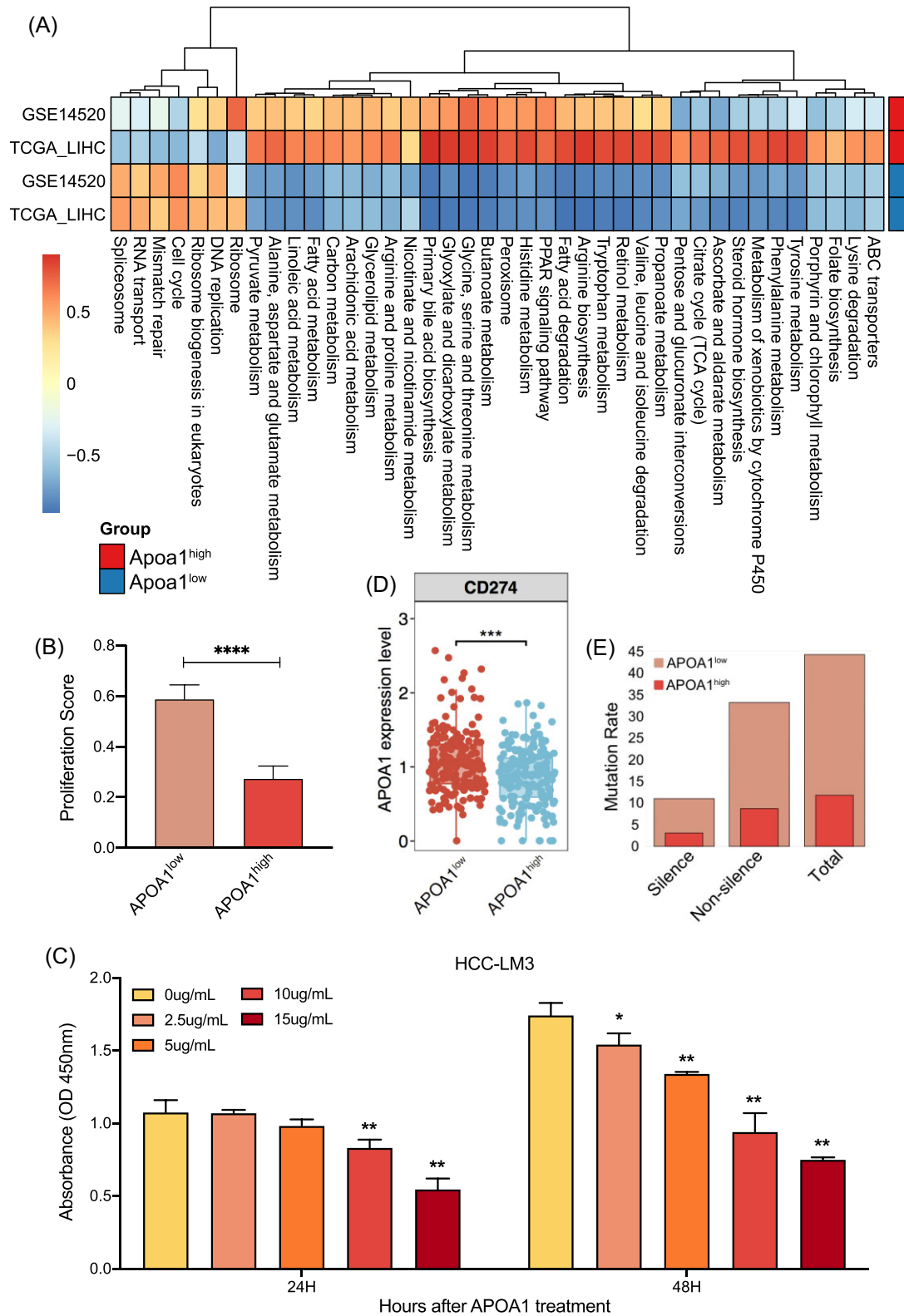


**Figure 7.** Differential pathways and mutation characteristics between APOA1<sup>high</sup> and APOA1<sup>low</sup> expression groups. **(A)** Hierarchical clustering of enriched pathways for differentially expressed genes between APOA1<sup>high</sup> and APOA1<sup>low</sup> expression groups. **(B)** Association analysis with proliferation score was performed between APOA1<sup>high</sup> and APOA1<sup>low</sup> expression groups (APOA1<sup>high</sup>, top 50%; APOA1<sup>low</sup>, bottom 50%). **(C)** HCC-LM3 cell proliferation assay. The x-axis represents the cell viability of HCC-LM3 cells treated with different APOA1 concentrations (0, 2.5, 5, 10, 15  $\mu$ g/ml) using the CCK-8 method for 24 and 48 h, and the y-axis represents the optical absorption value at a wavelength of 450 nm (\* $P < 0.05$ ; \*\* $P < 0.01$ ). **(D)** Differential analysis of the expression of immune checkpoint gene CD274 between APOA1<sup>high</sup> and APOA1<sup>low</sup> expression groups. **(E)** Difference in mutation rates, including silent and non-silent mutation rate, was compared between APOA1<sup>high</sup> and APOA1<sup>low</sup> expression groups (total: silence + non-silence).



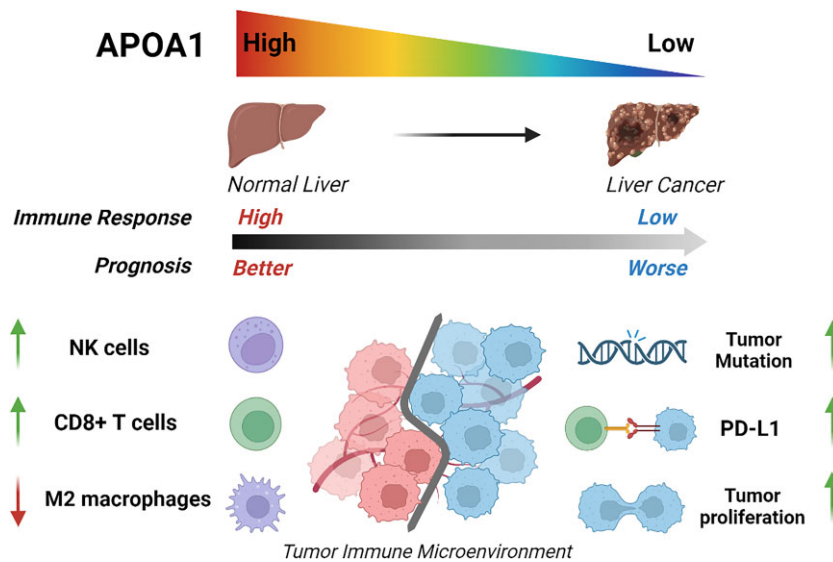


**Figure 8.** Top: influence of APOA1 on prognosis and TME of HCC. Bottom: overview of APOA1 in the prognosis and TME of HCC.

Considering the convenience and accuracy of serum APOA1 assay, APOA1 might be a very promising indicator for prognosis surveillance of HCC.

Then, the reason for the reduced expression of APOA1 in HCC was explored. DNA methylation is one of the most critical epigenetic signatures that is generally associated with transcriptional silencing.<sup>19</sup> In the present study, it was revealed that methylation levels of the APOA1 promoter region were significantly inversely correlated with APOA1 expression in tumor tissue, which might explain the reduction of APOA1. Furthermore, N<sup>6</sup>-methyladenosine (m6A) is the most abundant form of epigenetic modification of mRNAs and can mediate a variety of mRNA processes including translation, splicing, and mRNA degradation.<sup>20,21</sup> It was observed that the expression of m6A methylase-related genes was lower in the APOA1<sup>high</sup> group, which may indicate the transcriptional suppression of APOA1. It was also found that APOA1 expression and methylation levels do not have correlation in normal samples ( $r = -0.19$ ,  $P = 0.24$ ). From the perspective of data distribution, the distribution of the tumor and normal group in the methylation data is relatively consistent, while in the expression data, the data distribution of the two is quite different from that of methylation, which may be one of the reasons for the inconsistent conclusions drawn from the tumor and normal samples. Second, the methylation imbalance is one of the main characteristics of tumors, and hypermethylation in the promoter region leading to gene inactivation is an important feature of human tumors. Klutstein *et al.* pointed out that the aberrant methylation patterns commonly detected in cancer may have already been present in the normal cell prior to its transformation.<sup>22</sup> Some degree of methylation is not sufficient for carcinogenesis. Similarly, in our study, a certain level of methylation in the APOA1 promoter region was observed in the normal group. Since APOA1 is mainly expressed in hepatocytes, we believe that the methylation level of the promoter region is not the main mechanism regulating its expression under normal conditions.

The direct influence of APOA1 on cancer cells is still controversial since all previous results were based on either mouse or *in vitro* models. Data derived from HCC patients are needed to provide more precise information. Differential pathways and mutation characteristics of HCC between APOA1<sup>high</sup> and APOA1<sup>low</sup>

subgroups were investigated to uncover the influence of APOA1 on tumorigenesis. It was observed that tumors with a low level of APOA1 showed significantly higher enrichment of cell cycling, DNA replication, and mismatch repair pathways (Fig. 7). This study further screened out those genes expressions negatively correlated with APOA1 expression ( $R < -0.3$  and  $P < 0.05$ ), of which TP53BP1 is found both in two datasets (TCGA-LIHC and GSE14520). Enrichment of the “TP53 Regulates Transcription of DNA Repair Genes” pathway was identified from the Reactome database. Wang *et al.* found that the cytotoxic CD8 T cells 4 subset in HCC scRNA data showed considerable differences between the TP53 mutant and non-mutant groups, and 10 central genes were found, including APOA1.<sup>23</sup> All these results suggest that there is an important relationship between APOA1, TP53, and DNA repair pathways, which may be a new direction of targeted therapy in the future. On the other hand, the APOA1<sup>high</sup> subgroup showed less proliferation of tumor cells. This served to support APOA1 treatment of human HCC cell lines as an inhibitor of cancer cell proliferation by arresting the cell cycle. Moreover, higher tumor mutation rates in the APOA1<sup>low</sup> subgroup further suggested the protective mechanism of APOA1 against carcinoma development, accounting for the worse survival of patients with a low level of APOA1. The higher tumor mutational burden has been revealed to be associated with a worse prognosis in hepatocellular carcinoma,<sup>24</sup> and tumor mutational burden exerts a negative effect on immune cells within the TME.<sup>25</sup> These results support that APOA1 has a direct impact on HCC. While several previous reports showed that APOA1 did not exhibit a significant direct inhibitory effect on tumor cells, this may be because the tumor cell lines used *in vitro* were not human HCC cells.<sup>10,11</sup>

The TME is a complicated entity that in addition to tumor cells also consists of various immune cells that can either suppress neoplasm formation or promote tumorigenesis.<sup>26</sup> This study discovered that APOA1 expression was positively associated with immune infiltration of human CD8<sup>+</sup> T cells and NK cells in the TME. This observation aligns with the mouse model study showing that APOA1 promotes tumor infiltration of cytotoxic CD8<sup>+</sup> T cells.<sup>10</sup> APOA1-XGOF indicated that the most recognized function of APOA1 is cholesterol efflux and T cell cholesterol efflux pathways that can suppress T cell apoptosis and senescence.<sup>27</sup> It is

therefore plausible that a high APOA1 level is beneficial for the accumulation of CD8<sup>+</sup> T cells. As the most powerful effector cells responsible for the anticancer immune response,<sup>28</sup> the increased infiltration of CD8<sup>+</sup> T cells in HCC is, in general, considered to be a sign of good prognosis.<sup>29</sup>

Of note, another novel discovery is that APOA1 is mainly expressed in NK cells (Fig. 5A,B). As IFN $\gamma$  is a key cytokine that NK cells produce to kill cancer cells, NK cells were further annotated in seven subtypes by integrating the results of our analysis with the TISCH database. It was found that APOA1 expression was higher in NK-C3-IFN $\gamma$  in the normal group than in the tumor and blood groups (Figure S3C). The expression of APOA1 was identified on NK cells releasing IFN $\gamma$ , but there is no direct evidence to prove that there is a positive expression correlation between them. On the other hand, NK cells act as one of the main players in innate immunity against cancer, causing natural cytotoxicity against tumor cells and metastasis by preventing proliferation, migration, and colonization to distant regions.<sup>30</sup> NK cells preferentially utilize glucose which powers their effector functions and rapid proliferation, and limiting glucose can negatively impact NK cells' effector functions.<sup>31,32</sup> In contrast, the increased uptake of fatty acids is associated with NK cell dysfunction.<sup>33</sup> Since APOA1 exerts a significant influence on the processes of glucose metabolism<sup>34</sup> and cholesterol efflux, therefore it might interpret the positive relationship between APOA1 and NK cells and the lower APOA1 level in NK cells from tumors. Although the APOA1 fingerprint from an early omics analysis study suggested that APOA1 might be involved in the negative regulation of the immune effector process,<sup>35</sup> the present study refuted this conclusion and revealed that a high level of APOA1 can promote both adaptive immunity and innate immune response.

Furthermore, APOA1 expression was inversely correlated with the infiltration of CAFs, MDSCs, and M2 macrophages, further confirming the favorable immunoregulatory ability of APOA1 in HCC TME. CAFs, MDSCs, and M2 macrophages are prominent immunosuppressive cells able to reduce tumor cytotoxic T cell activity and secrete various effector molecules, thus contributing to an immunosuppressive TME and promoting tumor immune escape.<sup>36–38</sup> The above results indicate the vital role of APOA1 in regulating the antitumor immune response via direct or indirect ways, which all contribute to a more favorable TME with a stronger antitumor immune response.

In conclusion, this multi-dimensional study provides a comprehensive insight into the negative effect of APOA1 on tumor cell proliferation and tumor mutation burden, and its positive influence on the landscape of immune cells within the TME of HCC. In addition, it evaluates the potential of APOA1 as a prognostic indicator and elucidates the mechanism underlying APOA1 reduction in HCC. Therefore, in addition to its merit as a prognostic biomarker, APOA1 might be a viable therapeutic agent for cancer treatment to inhibit tumorigenicity and increase the antitumor immune response.

## Supplementary data

Supplementary data is available at *PCMEDJ Journal* online.

## Acknowledgments

This work was supported by the Innovation Group Project of Shanghai Municipal Health Commission (Grant No. 2019CXJQ03), the National Natural Science Foundation of China (Grants No. 31601075, 81972914, 81573023) and Shanghai “Rising Stars of Med-

ical Talent” Youth Development Program (Grant No. 2019–72). We would like to sincerely thank all the patients who participated in this research. In addition, we are also grateful to Shanghai Amplicon-gene Bioscience Co., Ltd, for their technical assistance in this study.

## Ethics statement

The studies involving human participants were reviewed and approved by the Institutional Ethics Committee of the leading medical center (Shanghai Eastern Hepatobiliary Surgery Hospital, EHBHKEY2020-02-012). The patients/participants provided their written informed consent to participate in this study.

## Conflict of interest

The authors disclose no conflicts of interest.

## Author contributions

Y.W. and S.P.C. performed methodology, investigation, and analysis and drafted the manuscript. X.X., F.Y., J.H.W., H.Z. and Y.Z.G. provided technique assistance. C.J.H., X.W.X. and M.F. checked the results and revised the manuscript. Y.W., X.Y.Z. and C.F.G. obtained the funding, supervised the data analysis, and coordinated the overall study. All authors have read and agreed to the published version of the manuscript.

## References

1. Forner A, Reig M, Bruix J. Hepatocellular carcinoma. *Lancet* 2018;**391**:1301–14. [https://doi.org/10.1016/S0140-6736\(18\)30010-2](https://doi.org/10.1016/S0140-6736(18)30010-2).
2. Yang JD, Hainaut P, Gores GJ, et al. A global view of hepatocellular carcinoma: Trends, risk, prevention and management. *Nat Rev Gastroenterol Hepatol* 2019;**16**:589–604. <https://doi.org/10.1038/s41575-019-0186-y>.
3. Llovet JM, Kelley RK, Villanueva A, et al. Hepatocellular carcinoma. *Nat Rev Dis Prim* 2021 **71** 2021;**7**:1–28. <https://doi.org/10.1038/s41572-020-00240-3>.
4. Yang C, Zhang H, Zhang L, et al. Evolving therapeutic landscape of advanced hepatocellular carcinoma. *Nat Rev Gastroenterol Hepatol* 2022;**20**:1–20. <https://doi.org/10.1038/s41575-022-00704-9>.
5. Tandon P, Garcia-Tsao G. Prognostic indicators in hepatocellular carcinoma: A systematic review of 72 studies. *Liver Int* 2009;**29**:502–10. <https://doi.org/10.1111/J.1478-3231.2008.01957.X>.
6. Wang Y, Tong Y, Zhang Z, et al. ViMIC: A database of human disease-related virus mutations, integration sites and cis-effects. *Nucleic Acids Res* 2022;**50**:D918–27. <https://doi.org/10.1093/NAR/GKAB779>.
7. Mustafa MG, Petersen JR, Ju H, et al. Biomarker discovery for early detection of hepatocellular carcinoma in hepatitis C-infected patients. *Mol Cell Proteomics* 2013;**12**:3640–52. <https://doi.org/10.1074/MCP.M113.031252/ATTACHMENT/6.A22F44C-96F5-420E-BB2A-CF39CEEB4B57/MMC1.PDF>.
8. Ma XL, Gao XH, Gong ZJ, et al. Apolipoprotein A1: A novel serum biomarker for predicting the prognosis of hepatocellular carcinoma after curative resection. *Oncotarget* 2016;**7**:70654–68. <https://doi.org/10.18632/ONCOTARGET.12203>.
9. Ni XC, Yi Y, Fu YP, et al. Role of lipids and apolipoproteins in predicting the prognosis of hepatocellular carcinoma after re-

- section. *Onco Targets Ther* 2020;**13**:12867–80. <https://doi.org/10.2147/OTT.S279997>.
10. Zamanian-Daryoush M, Lindner D, Tallant TC, et al. The cardioprotective protein apolipoprotein a1 promotes potent anti-tumorigenic effects. *J Biol Chem* 2013;**288**:21237–52. <https://doi.org/10.1074/JBC.M113.468967/ATTACHMENT/561D2C70-C8C3-467B-87FF-5FD81F30B328/MMC1.DOC>.
  11. Peng M, Zhang Q, Cheng Y, et al. Apolipoprotein A-I mimetic peptide 4F suppresses tumor-associated macrophages and pancreatic cancer progression. *Oncotarget* 2017;**8**:99693. <https://doi.org/10.18632/ONCOTARGET.21157>.
  12. Duan Q, Zhang H, Zheng J, et al. Turning cold into hot: Firing up the tumor microenvironment. *Trends Cancer* 2020;**6**:605–18. <https://doi.org/10.1016/j.TRECAN.2020.02.022>.
  13. Chen S, Gao Y, Wang Y, et al. The combined signatures of hypoxia and cellular landscape provides a prognostic and therapeutic biomarker in hepatitis B virus-related hepatocellular carcinoma. *Int J Cancer* 2022;**151**:809–24. <https://doi.org/10.1002/IJC.34045>.
  14. Binnewies M, Roberts EW, Kersten K, et al. Understanding the tumor immune microenvironment (TIME) for effective therapy. *Nat Med* 2018 245 2018;**24**:541–50. <https://doi.org/10.1038/s41591-018-0014-x>.
  15. Genard G, Lucas S, Michiels C. Reprogramming of tumor-associated macrophages with anticancer therapies: Radiotherapy versus chemo- and immunotherapies. *Front Immunol* 2017;**8**:828. <https://doi.org/10.3389/FIMMU.2017.00828>.
  16. Wang Y, Zong H, Yang F, et al. A knowledge empowered explainable gene ontology fingerprint approach to improve gene functional explication and prediction. *ISCIENCE* 2023;**26**:106356. <https://doi.org/10.1016/j.isci.2023.106356>.
  17. Thorsson V, Gibbs DL, Brown SD, et al. The Immune Landscape of cancer. *Immunity* 2018;**48**:812–30. <https://doi.org/10.1016/j.IMMUNI.2018.03.023/ATTACHMENT/8D3FFC74-4DB4-4531-A4AD-389DFC8BB7EC/MMC7.XLSX>.
  18. Chen M, Wei L, Law CT, et al. RNA N6-methyladenosine methyltransferase-like 3 promotes liver cancer progression through YTHDF2-dependent posttranscriptional silencing of SOCS2. *Hepatology* 2018;**67**:2254–70. <https://doi.org/10.1002/HEP.29683/SUPPINFO>.
  19. Dhar GA, Saha S, Mitra P, et al. DNA methylation and regulation of gene expression: Guardian of our health. *Nucl* 2021;**64**:259–70. <https://doi.org/10.1007/S12327-021-00367-Y/TABLES/1>.
  20. Slobodin B, Han R, Calderone V, et al. Transcription impacts the efficiency of mRNA translation via Co-transcriptional N6-adenosine methylation. *Cell* 2017;**169**:326–37. <https://doi.org/10.1016/j.cell.2017.03.031>.
  21. Shi H, Wei J, He C. Where, when, and how: Context-dependent functions of RNA methylation writers, readers, and erasers. *Mol Cell* 2019;**74**:640–50. <https://doi.org/10.1016/J.MOLCEL.2019.04.025>.
  22. Klutstein M, Nejman D, Greenfield R, et al. DNA methylation in cancer and aging. *Cancer Res* 2016;**76**:3446–50. <https://doi.org/10.1158/0008-5472.CAN-15-3278>.
  23. Wang H, Fu Y, Da BB, et al. Single-cell sequencing identifies the heterogeneity of CD8+ T cells and novel biomarker genes in hepatocellular carcinoma. *J Healthc Eng* 2022;**2022**:8256314. <https://doi.org/10.1155/2022/8256314>.
  24. Xie F, Bai Y, Yang X, et al. Comprehensive analysis of tumour mutation burden and the immune microenvironment in hepatocellular carcinoma. *Int Immunopharmacol* 2020;**89**:107135. <https://doi.org/10.1016/J.INTIMP.2020.107135>.
  25. Zhou W, Fang D, He Y, et al. Correlation analysis of tumor mutation burden of hepatocellular carcinoma based on data mining. *J Gastrointest Oncol* 2021;**12**:1117–31. <https://doi.org/10.21037/JGO-21-259>.
  26. Anderson NM, Simon MC. The tumor microenvironment. *Curr Biol* 2020;**30**:R921–5. <https://doi.org/10.1016/j.cub.2020.06.081>.
  27. Bazioti V, La Rose AM, Maassen S, et al. T cell cholesterol efflux suppresses apoptosis and senescence and increases atherosclerosis in middle aged mice. *Nat Commun* 2022;**13**:1–23. <https://doi.org/10.1038/s41467-022-31135-4>.
  28. Raskov H, Orhan A, Christensen JP, et al. Cytotoxic CD8+ T cells in cancer and cancer immunotherapy. *Br J Cancer* 2020;**124**:359–67. <https://doi.org/10.1038/s41416-020-01048-4>.
  29. Bian J, Lin J, Long J, et al. T lymphocytes in hepatocellular carcinoma immune microenvironment: Insights into human immunology and immunotherapy. *Am J Cancer Res* 2020;**10**:4585.
  30. Wu SY, Fu T, Jiang YZ, et al. Natural killer cells in cancer biology and therapy. *Mol Cancer* 2020;**19**:1–26. <https://doi.org/10.1186/S12943-020-01238-X/TABLES/3>.
  31. Assmann N, O'Brien KL, Donnelly RP, et al. Srebp-controlled glucose metabolism is essential for NK cell functional responses. *Nat Immunol* 2017;**18**:1197–206. <https://doi.org/10.1038/ni.3838>.
  32. Mah AY, Rashidi A, Keppel MP, et al. Glycolytic requirement for NK cell cytotoxicity and cytomegalovirus control. *JCI Insight* 2017;**2**:e95128. <https://doi.org/10.1172/JCI.INSIGHT.95128>.
  33. Kobayashi T, Lam PY, Jiang H, et al. Increased lipid metabolism impairs NK cell function and mediates adaptation to the lymphoma environment. *Blood* 2020;**136**:3004–17. <https://doi.org/10.1182/BLOOD.2020005602>.
  34. Drew BG, Rye KA, Duffy SJ, et al. The emerging role of HDL in glucose metabolism. *Nat Rev Endocrinol* 2012;**8**:237–45. <https://doi.org/10.1038/nrendo.2011.235>.
  35. Ardakani MJE, Safaei A, Oskouie AA, et al. Evaluation of liver cirrhosis and hepatocellular carcinoma using Protein-Protein Interaction Networks. *Gastroenterol Hepatol Bed Bench* 2016;**9**:S14.
  36. Mao X, Xu J, Wang W, et al. Crosstalk between cancer-associated fibroblasts and immune cells in the tumor microenvironment: New findings and future perspectives. *Mol Cancer* 2021;**20**:1–30. <https://doi.org/10.1186/S12943-021-01428-1>.
  37. Gabrilovich DI, Nagaraj S. Myeloid-derived suppressor cells as regulators of the immune system. *Nat Rev Immunol* 2009;**9**:162–74. <https://doi.org/10.1038/nri2506>.
  38. Pittet MJ, Michielin O, Migliorini D. Clinical relevance of tumour-associated macrophages. *Nat Rev Clin Oncol* 2022;**19**:402–21. <https://doi.org/10.1038/s41571-022-00620-6>.